RSC Advances

ROYAL SOCIETY OF CHEMISTRY

www.rsc.org/advances

Simultaneous removal of NH_4^+-N and refractory organics through sequential heterogeneous Fenton oxidation process and struvite precipitation: Kinetic study

*P. Maharaja, E.Gokul, N.Prabhakaran, K.Patchai murugan, S. Karthikeyan, R.Boopathy, S. Swarnalatha and G. Sekaran**

Environmental Technology Division, Council of Scientific & Industrial Research (CSIR), Central Leather Research Institute (CLRI), Adyar, Chennai 600 020, India

*** Corresponding Author**

Dr. G. Sekaran,

Chief Scientist & Cluster chairman

Environmental Technology Division,

Central Leather Research Institute,

Adyar, Chennai – 600 020,

Tamil Nadu, India

Tel.: +91-44-24911386 (Extn: 7241)

Fax: +91-44-24452941

Email: ganesansekaran@gmail.com

Abbreviations

COD- Chemical Oxygen Demand

BOD-Biochemical Oxygen Demand

APHA-American Public Health Association

TOC-Total Organic Carbon

TKN- Total Kjeldhal Nitrogen

TGA- Thermo Gravimetric Analysis

DSC-Differential Scanning Colorimetry

DTA-Differential Thermal Analysis

XRD- X-Ray Diffraction Analysis

SEM-Scanning Electron Microscopy

FT-IR -Fourier Transform Infra Red Spectroscopy

UV-Vis Ultraviolet Visible Spectroscopy

MAP-Magnesium Ammonium Phosphate

NPAC- Nanoporous Activated Carbon

AOP-Advanced Oxidation Processes

HFO- Heterogeneous Fenton Oxidation

HRT- Hydraulic Retention Time

ANWW - Ammoniacal nitrogen containing wastewater

$[ANWW]_{HFO}$ - Ammoniacal nitrogen containing wastewater after heterogeneous fenton oxidation process

Abstract

The aim of the present investigation was to treat wastewater containing high concentration of NH_4^+ -N by Heterogeneous Fenton oxidation of organics and struvite precipitation. The Fenton reagent (Fe^{2+}/H_2O_2-10mM/9.8mM) and Nanoporous Activated Carbon (30 g/L) as the heterogeneous matrix were used in heterogeneous Fenton oxidation (HFO) process for the destruction of refractory organic compounds present in Ammoniacal nitrogen containing wastewater (ANWW). The HFO process was followed by NH_4^+- N removal from the ANWW as struvite crystals using MgO and $Na_2HPO_4 \cdot 2H_2O$. The maximum removal of NH_4^+ -N as struvite was achieved by 96% at solution pH, 9.0 and at ambient temperature after the destruction of organic compounds by HFO process. The optimum time for struvite precipitation was 60min and secondary crystallization time for struvite crystals was 2 h. The removal of organic impurities was confirmed through FT-IR analysis of struvite crystals formed with and without HFO treatment. The thermal stability of struvite crystals was evaluated by TGA and DTA analyses and enthalpy of formation of struvite was determined through DSC analysis. Orthorhombic crystalline nature of the struvite crystals recovered from ANWW and $[ANWW]_{HFO}$ was evaluated through XRD spectroscopy. The surface morphology of precipitated struvite was analysed using Scanning Electron Microscopy.

Keywords: Struvite crystals, Heterogeneous Fenton oxidation; NH_4^+ -N, Ammoniacal nitrogen containing wastewater, optimization of MAP precipitation

Introduction

Leather, textiles, pharmaceuticals and chemical industries discharge wastewater containing high concentration of nitrogen in the form of ammonia, nitrite and nitrate.[1,2] The direct discharge of high concentration of ammoniacal nitrogen deteriorated the receiving water quality and it also severely damaged the local ecology.[3] Therefore, it becomes necessary to eliminate these inorganic nitrogeneous compounds from the wastewater before entering into any aquatic systems. The available processes which possess practical importance can be broadly classified into two main categories such as biological processes and physico-chemical processes. The biological processes for the treatment of wastewater containing NH_4^+-N include nitrification-denitrification process and anammox process.[4,5] The excess addition of methanol to the system, the pH maintenance and high hydraulic retention time for the treatment of wastewater containing nitrogen were considered to be the major limitations of the biological treatment process.[6] Hence, only few processes are being exploited at the commercial scale**.** The physico-chemical processes involve stripping of NH_4^+ -N from the effluent by air or stream; the electrochemical conversion and ion exchange method were also reported for the treatment of ammoniacal nitrogen containing wastewater (ANWW).[7-10] The major limitations of these physico-chemical processes are high capital and operating costs and also the fact that the ammonia stripped out from ANWW contribute to air pollution.[11]

Magnesium ammonium phosphate precipitation (MAP process) is considered to be one of the most effective methods for the management of high NH_4^+-N containing wastewater. MAP is also known as struvite a crystalline substance containing magnesium, phosphate and ammonium ions at the equi molar ratio represented with molecular formula $MgNH_4PO_4.6H_2O$. Struvite may be regarded as a slow release kind

of fertilizer.[12-15] Moreover, Struvite would be the most alternative fertilizer for commercial crops such as sugar beet which needs magnesium content.[16] The pH plays an important role during the MAP precipitation process. Struvite or MAP may be precipitated at a wide range of alkaline pH (7.0–11.5), but the suitable pH ranges was found to be 7.5 to 9.0.[17-19] The precipitation of struvite takes place in the presence of magnesium (Mg^{2+}), ammonium (NH_4^+), and phosphate (PO_4^{3-}) ions as per the equation (1),

$$Mg^{2+} + NH_4^+ + PO_4^{3-} + 6H_2O \rightarrow MgNH_4PO_4.6H_2O \quad (1)$$

According to equation (1), Mg^{2+}, NH_4^+, and PO_4^{3-} are required to be in equi-molar quantities to form $MgNH_4PO_4.6H_2O$. However, certain chemical species present in aqueous solution consume Mg^{2+}, NH_4^+ and/or PO_4^{3-} compounds by isomorphous crystallization. Hence, precipitation of struvite needed additional Mg^{2+} and/or PO_4^{3-} higher than the stoichiometric ratio for the maximum yield.[20-22]

The struvite crystals recovered from the wastewater stream contains organic compounds as an inclusion and thus, the reuse of struvite crystals have limited applications.[17] Microwave irradiation dissociates the struvite into Mg^{2+}, NH_4^+, and PO_4^{3-} ions that are recycled again to the influent wastewaters for struvite precipitation that reduced the struvite production cost.[23] Therefore the usage of the struvite as the fertilizer or as the source of Magnesium ions and Phosphate ions for the recycling process recovered from the wastewater streams should be in the pure condition in order to prevent from the effect of organics present in the wastewater. Moreover, the presence of organics in wastewater retards the MAP precipitation result in poor removal efficiency. Thus, it is essential to eliminate the organic impurities from the wastewater to enhance the NH_4^+-N removal efficiency and to increase the purity of the struvite crystals.

Karthikeyan et. al.2012, has reported the removal of organic impurities from the NH_4^+-N containing tannery wastewater by heterogeneous Fenton oxidation process.[24] Hetero fenton oxidation (HFO) process consists of the catalytic oxidation of organics in wastewater by insitu generated hydroxyl radical, having high oxidation potential (2.8V), using nanoporous activated carbon as the heterogeneous catalyst. Hence, this present investigation was focused on the treatment of NH_4^+-N containing wastewater by integrated heterogeneous Fenton oxidation (HFO) of organics and followed by precipitation of ammonium ion as Magnesium ammonium phosphate (MAP) presented in Fig.1.

Materials and methods

Materials

All the chemicals used in the present study such as MgO, $Na_2HPO_4.2H_2O$, $FeSO_4.7H_2O$, Hydrogen peroxide (30% v/v) were of analytical grade purchased from Sigma-Aldrich, India.

Collection and characterization of wastewater

The ANWW was collected from a chemical industry cluster engaged in manufacturing of pigments, paints, dyestuff etc. located in Gujarat, India. The various physicochemical parameters were analysed by following the methods as detailed in Standard methods for analysis of water and wastewater.[25] The wastewater sample was pretreated to remove the coarse suspended solids by sand filtration. The characteristics of raw wastewater before and after sand filtration are presented in Table 1.

Preparation of Nanoporous Activated Carbon (NPAC)

The heterogeneous catalyst, NPAC was prepared from rice husk, the agricultural solid waste.The procedure followed for the preparation of nanoporous activated carbon

(NPAC) was described in detail by the authors in their previous publication.[26] NPAC was prepared by two sequential steps such as pre-carbonization and chemical activation. The washed rice husk was packed in an air-tight graphite crucible and pre-carbonized at 400°C for 4h. The pre-carbonized material was activated using ortho phosphoric acid (H_3PO_4) at 800°C at a heating rate of 5°C/min. The activated carbon was further oxidized using 5M Nitric acid (HNO_3) at 60°C for 3 h. The NPAC on oxidation with nitric acid was imparted with oxygenated functional groups such as –COOH, -OH and C=O on the surface of the matrix. The oxidized NPAC was washed with acid/alkali to get neutral condition The oxidized NPAC was dried at 110°C in hot air oven for 4 hours to drive away the moisture and it was designated as NPAC.

Characterization of NPAC catalyst and MAP product

NPAC was characterized for surface area, pore volume and pore size distribution by automatic adsorption instrument (Quantachrome Corporation, USA). The elemental composition (Carbon, Hydrogen and Nitrogen content) of the NPAC was determined using Vario MICRO CHNSO 15091002 (Carlo–Erba analyser, Germany). FT-IR Spectroscopy (Perkin-Elmer, USA) was used for the investigation of the surface functional groups in MAP. Spectral analysis was recorded in the range 4000 - 400 cm^{-1}. MAP samples (0.1 g) were homogenised with KBr (1g) of spectroscopy grade (Merk, Darmstadt, Germany) in a mortar. The crystalline nature of MAP precipitate was determined by X-ray diffraction (XRD) analysis in Rich Siefert 3000 diffractometer using Cu-$K_\alpha 1$ radiation (λ= 0.1541 nm). The morphology of MAP samples recovered from ANWW and $[ANWW]_{HFO}$ were evaluated by SEM analysis. The SEM analysis was performed using a scanning device attached to a JEOL JM 5600 electron microscope at 20 kV (JEOL, Japan) accelerating voltag e with a 5–6-nm electron beam. Thermo Gravimetric Analysis (TGA) and Differential Scanning Calorimetric (DSC)

analysis were carried out from 30 to 800°C with a temperature gradient of 10 °C min^{-1} under a nitrogen atmosphere and scans were recorded using a TGA Q50 (V20.6 Build 31, USA).

Characteristics of NPAC

The NPAC was selected as a heterogeneous catalyst for the oxidation of dissolved organics in wastewater for its endowed characteristics such as surface area, 379 m^2 /g; pore volume, 0.188 cm^3 /g; pore diameter, 39.36 Å; C, 41.5%; H, 2.85%; N, 0.7%; and free electron density , 1.60×10^{22} spins/g. The maximum reflectance measured at λ_{800}nm in UV-Visible spectrophotometer correlates with the energy gap (Eg) of 1.55 eV for NPAC which explains the extrinsic semiconductor property of NPAC.[25]

Characterization of Ammoniacal nitrogen containing wastewater (ANWW)

The ANWW and $[ANWW]_{HFO}$ samples were characterised for Chemical Oxygen Demand COD), Biochemical Oxygen Demand (BOD_5) as per standard methods described in APHA (1995). The NH_4^+-N and Total Kjeldhal Nitrogen (TKN) of wastewater samples were determined by Kjeldhal distillation method using Buchi distillation Unit K-350 (BUCHI, Switzerland). The pH of the solution was measured using precalibrated pH meter (Systronics 620, India). Total organic carbon (TOC) was analysed by TOC analyser (SHIMADZU Model no: SHIMADZU CORP 00291, India). The TOC analyzer was calibrated using potassium hydrogen phthalate at 1000 ppm as standard TOC solution.

Heterogeneous Fenton Oxidation (HFO) process

The heterogeneous Fenton oxidation process was used for the treatment of ANWW. In this study, Fe^{2+}/H_2O_2 was selected as Fenton reagent and NPAC (30 g/L) as the heterogeneous catalyst for the destruction organic compounds in wastewater.[27-28]

The experiment was carried out by taking one litre of ANWW sample in a fluidized bed reactor (10.2 cm x 10.2 cm x 22.4 cm dimension) with the total volume of 1.4L. Fenton reagent, a mixture of hydrogen peroxide H_2O_2, (9.8 mM) and $FeSO_4.7H_20$ (10mM) was used for the oxidation of refractory organics in wastewater. The hydroxyl radicals are generated from fenton reagent (ferrous ion and hydrogen peroxide) as per the following equations.

$$H_2O_2 + Fe^{2+} \rightarrow {}^{\bullet}OH + OH^- + Fe^{3+} \quad (2)$$

$$Fe^{3+} + H_2O_2 \rightarrow Fe^{2+} + HO_2^{\bullet} + H^+ \quad (3)$$

The hydroxyl radical is also generated from NPAC and molecular oxygen in HFO process. The electron transfer from electron rich NPAC to molecular oxygen generate reactive oxygen species (equation 4) which is considered to be the primary step in formation of hydroxyl radical with NPAC.[26]

$$NPAC(e_{cb}^-) + O_2 \rightarrow NPAC(O_2^{\bullet})_{ads} \quad (4)$$

The formation of hydroxyl radical from the reactive oxygen species in adsorbed state takes place as explained in equations (5) and (6).

$$NPAC(h_{vb}^+) + H_2O \rightarrow NPAC({}^{\bullet}OH)_{ads} + H_{aq}^+ \quad (5)$$

$$NPAC(O_2^{\bullet})_{ads} + H_{aq}^+ \rightarrow NPAC(2{}^{\bullet}OH)_{ads} \quad (6)$$

The hydroxyl radicals react with the organic pollutants in the wastewater in shorter time and convert them into smaller and biodegradable organic compounds. At the end of the complete chemical reaction, the system is left behind with carbon dioxide, water and fragmented organic compounds with low molecular weights according to the equation (7).

$${}^{\bullet}OH + \text{Refractory organiccompounds} \rightarrow \text{Oxidizedcompounds} + CO_2 + H_2O \quad (7)$$

Initially, the ANWW was filtered at its native pH 0.82 through sand filter to remove suspended solids. The HFO process was carried out by taking 1 litre sand filtered ANWW at its pH, 0.87. Fenton reagent (H_2O_2 : Fe^{2+} at 9.8mM: 10mM) and NPAC(30g/L) were added to the fluidized bed reactor and the contents were fluidized by compressed air at 2.0 kg/cm^2 pressure supplied through air sparger provided at the bottom of the reactor. The oxidation of organics in ANWW was carried out at ambient conditions. The samples were periodically collected at different time intervals (2, 4, 6, 8 and 10 h) from the HFO reactor for the characterisation of BOD and COD. The Heterogeneous Fenton oxidised ammoniacal nitrogen containing wastewater was named as $[ANWW]_{HFO}$.

MAP precipitation

The precipitation of NH_4^+-N from ANWW as struvite was carried out by adjusting the ANWW and $[ANWW]_{HFO}$ pH to 7.0 using sodium hydroxide (10% w/v). The sequential addition of MAP reagents was in the order of phosphate source ($Na_2HPO_4.2H_2O$) followed by magnesium oxide (MgO) and the solution was agitated at 50 rpm for 60 min using magnetic stirrer. The secondary crystallization of struvite was allowed for 2 h and the NH_4^+-N free wastewater was separated by filtration using glass microfiber filter paper (0.45 µm, GF/A). The experiment was repeated at different reaction time periods such as 60, 90 and 120 min as the rate of agitation and the solution pH play a significant role in the formation of nuclei in struvite precipitation.[17,29] The supernatant solution after settling the struvite crystals was collected and characterized for NH_4^+-N to evaluate the removal efficiency. The molar ratio of MAP reagents (MgO and $Na_2HPO_4.2H_2O$) was varied for the optimization of maximum removal of NH_4^+- N present in the wastewater. The integrated heterogeneous Fenton oxidation and struvite precipitation process is shown in Fig. 2.

Results and Discussion

Treatment efficiency and formation of struvite precipitate

The removal efficiency of NH_4^+- N and purity of the recovered struvite in the integrated process were evaluated.

Heterogeneous Fenton oxidation (HFO) process

Effect of time

The effect of time on HFO process for the maximum removal of organic compounds from the ANWW sample interms of percentage removal of COD is shown in Fig. 3. The maximum COD removal was achieved at 6 h reaction time and no significant changes in COD was observed with increase in reaction time up to 10 h. The COD removal increased steadily with time upto 6 h and followed by non linear section. Hence, the reaction time in HFO process was optimized to be 6 h. A set of experiments were also carried out in the presence of NPAC catalyst with and without fenton reagent to confirm that the removal of organic compounds was due to adsorption or oxidation. It was observed that the reduction in COD was only 15 % in the absence of fenton reagent.

Kinetic study for HFO process:

The kinetics on the removal of organics by HFO process was studied by applying pseudo first order and pseudo second order kinetic models as expressed in eqns(8) and (9),

$$\ln COD_t / COD_0 = -k_1 t \quad (8)$$

$$1/ COD_t = 1/ COD_0 + k_2 t \quad (9)$$

where, COD_0 is initial COD (mg/L), COD_t is COD (mg/L) at time t, k_1 and k_2 are the pseudo first and pseudo second order rate constants.

The kinetic study of the HFO process was carried out and the results are shown in Fig. 4 (a) and Fig 4(b). The results illustrate that the COD removal by HFO process was best obeyed the pseudo second order rate kinetic model with regression coefficient value of 0.997 and χ^2 value of 0.0023 as shown in Table 2. This indicated that the rate of the reaction depend upon the Fenton reagent and NPAC/O_2 for the removal of refractory organics present in ANWW during HFO process.

An increase in the solution pH after the addition of MAP reagents increased the crystal growth by supersaturation.[30] Generally, the formation of struvite crystals depends on reactant concentration and solution pH. As mentioned above struvite or MAP may be precipitated in the wide range of alkaline pH (7.0–11.5), but the suitable pH ranges was found to be 7.5 to 9.0.[17-19] This may be due to decrease in solubility of struvite with the increase in solution pH. In the present investigation, the struvite precipitation was performed at pH 7.0 after HFO process. The struvite precipitation was initiated by the addition of $Na_2HPO_4.2H_2O$ at the required molar ratio (1.0 to 1.5), and it was followed by the addition of another MAP reagent, MgO at required molar ratio (1.0 to 1.5). Table 3 shows that the increase in molar ratio of MAP reagents from 1.0 to 1.5 increased the solution pH significantly.

After the addition of two MAP reagents the solution pH was adjusted to different alkaline pH (8.5 to 10.5) using sodium hydroxide (10% w/v) for the secondary struvite crystallization. The results revealed that the maximum removal of NH_4^+-N was observed at pH 9.0 and thereafter the removal efficiency of NH_4^+-N was not increased significantly. Hence, the optimum solution pH for the maximum struvite precipitation

was fixed at 9.0. The secondary struvite crystallization enhanced the NH_4^+- N removal by 20-25% and it completed the struvite formation process.

MAP precipitation after the organic removal by HFO process

The MAP precipitation was carried out in the following four steps:

(i) The destruction of organic compounds by heterogeneous Fenton oxidation process by the Fenton reagent (Fe^{2+}/H_2O_2) in the presence of nanoporous activated carbon (NPAC) as the heterogeneous catalyst.

(ii) The pH was increased to 7.0 using sodium hydroxide (10% w/v)

(iii) MAP precipitation was carried out using the precipitating reagents (MgO and $Na_2HPO_4.2H_2O$).

(iv) Secondary struvite crystallization by increase the pH up to 9 using sodium hydroxide (10% w/v)

The HFO process destructs the organic pollutants in the wastewater using hydroxyl radicals generated from Fenton reagent and from NPAC/O_2 at its working condition. The NPAC plays the important role in the production of hydroxyl radicals and subsequent oxidation of organic compounds in wastewater.[28] The nanoporous network structure present in NPAC adsorbs and destruct organic molecules in the wastewater by insitu generated hydroxyl radicals.[27] In the present investigation, the COD removal was in the range 52-55% due to the presence of refractory organic chemicals and high TDS or may be due to partial oxidation of organics present in wastewater.

The struvite crystals recovered from $[ANWW]_{HFO}$, named Struvite I, was found to have high purity than the purity of struvite crystals recovered from ANWW, named struvite II. This confirmed that the integrated HFO process enabled the recovery of struvite crystals with high purity. After HFO treatment the pH of the solution was adjusted to 7.0 using sodium hydroxide (10% w/v).The precipitation of struvite was

optimized by varying the concentration of MAP reagents (MgO and $Na_2HPO_4.2H_2O$) at the stoichiometric molar ratio of 1:1:1, 1:1:1.1, 1:1.2:1.2, 1:1.3:1.3, 1:1.4:1.4 and 1:1.5:1.5 at ambient conditions with respect to Mg^{2+}:NH_4^+:PO_4^{3-} composition. Then, the pH of the solution was increased up to 9 using sodium hydroxide (10% w/v) for secondary crystallization of struvite crystals.

Fig. 5(a-d) show that the NH_4^+-N was removed by 86.5% -96.4% along with COD reduction by 63.8% -78.2%; BOD by 49.4% - 69.8% and TOC by 51.9%-54.5% during struvite precipitation from $[ANWW]_{HFO}$. The percentage removal of NH_4^+-N increased with increase in molar ratio of precipitating reagents until it reached the stoichiometric molar ratio of 1:1.4:1.4. Many researchers reported that the formation of struvite occurred at the equi molar concentrations (1:1:1) of Mg^{2+}, NH_4^+, and PO_4^{3-} species. The consumption of the precipitating reagents higher than the stoichiometric molar ratio of struvite formation due to the presence of other ionic reactants. Further increase in the ratio does not influence on the reduction of NH_4^+-N. Hence, the optimum stoichiometric molar ratio was selected as 1:1.4:1.4 for the maximum removal of NH_4^+-N. The reduction percentage was not increased as the noticeable amount continuously after increase the stoichiometric molar ratio of 1:1.5:1.5 and above.

MAP precipitation in the absence of HFO process

This study was carried out by the following three steps:

(i) Adjustment of initial ANWW pH to 7.0 using sodium hydroxide (10% w/v)

(ii) MAP precipitation was carried out using $Na_2HPO_4.2H_2O$ and MgO.

(iii) Secondary struvite crystallization by increase the pH up to 9 using sodium hydroxide (10% w/v)

The precipitation of struvite crystals using precipitating reagents (MgO and $Na_2HPO_4.2H_2O$) at different stoichiometric molar ratio of Mg^{2+}:NH_{4+}:PO_{43}^- such as

1:1:1, 1:1:1.1, 1:1.2:1.2, 1:1.3:1.3, 1:1.4:1.4 and 1:1.5:1.5 at ambient conditions. Then, the pH of the solution was increased up to 9 in secondary crystallization of struvite crystals.

The Fig. 5(a-d) show that the overall removal of efficiency of NH_4^+-N was found to be 76.9% - 84.1% along with the reduction in COD by 42.4% - 49.6%; BOD by 27.4% - 43.0% and TOC by 19.3% - 23.1%. The percentage removal of NH_4^+-N and other pollutants increased with increase in concentration of precipitating reagents (MgO and $Na_2HPO_4.2H_2O$) up to the stoichiometric molar ratio of 1:1.5:1.5 thereafter the removal of organic content remained the same.

Kinetic study on Struvite precipitation after Heterogeneous Fenton Oxidation of organics in wastewater

The kinetics on the formation of struvite crystals was studied by applying pseudo-first order and pseudo-second order kinetic models as expressed in eqns (10) and (11),

$$\ln \{[NH_4^+\text{-}N]_t / [NH_4^+\text{-}N]_0\} = -k_1 t \quad (10)$$

$$1/ [NH_4^+\text{-}N]_t = 1/ [NH_4^+\text{-}N]_0 + k_2 t \quad (11)$$

where, $[NH_4^+\text{-}N]_0$ is concentration of initial NH_4^+-N (mg/L), $[NH_4^+\text{-}N]_t$ is concentration of NH_4^+-N (mg/L) at time t, k_1 and k_2 are the pseudo-first and pseudo-second order rate constants.

The results on the kinetic study on struvite precipitation after HFO process are presented in Fig. 6(a) and 6(b). The results illustrate that the precipitation of struvite were best obeyed to second order rate kinetic model with regression coefficient 0.987 and $\chi 2$, 0.0026 as shown in Table 4. Ohlinger et al.[28] studied the MAP process for phosphate removal from anaerobic lagoon effluent and it was reported that the formation of struvite obeyed first order kinetic model with rate constant 4.2 h^{-1}. Nelson

et al.[14] also reported the first order kinetics with the rate constant 12.3 h^{-1} (at pH 9.0) for phosphorus removal from anaerobic swine lagoon effluent as struvite. Turker et al., [31] reported that the formation of struvite follows the second order rate kinetics for the removal of ammonia from anaerobic digester effluents. But, in the present investigation struvite precipitation was limited by the concentration of MAP reagents, hence the kinetics for the removal of NH_4^+-N followed pseudo-second order rate kinetic model. The calculated pseudo-second order rate constant was found to be 0.365 litre mol^{-1} min^{-1}.

Characterization of recovered struvite by instrumentation techniques

TGA and DSC analyses

TGA analysis is used to evaluate the presence of volatile constituents, thermal stability, decomposition characteristics, ageing/breakdown, sintering behaviour and reaction kinetics of the solid samples. Fig. 7(a) and 7(b) show the thermal stability of the recovered struvite crystals I and II. The study was performed from room temperature to 850 °C. The weight loss up to temperature 180 ºC is due to the evaporation of NH_3 and H_2O molecules. The struvite crystals recovered from ANWW and $[ANWW]_{HFO}$ were recorded a high percentage of weight loss by 50.41% and 51.6 % respectively. This corresponds with the values reported by many researchers on struvite crystals recovery under different processes.[32-34]

The activation energy (E_a) was calculated from TGA thermograms of Struvite-I and Struvite-II by using the following equation (12),

$$\ln[(dw/dt/w)]=\ln A-E_a/2.303RT \quad (12)$$

where, dw/dt is the weight loss with respect to time; w is the initial weight of the struvite considered for TGA analysis ;A is the exponential factor;R is gas constant and

T is the temperature in K.The activation energy for the formation of Struvite-I was calculated as 1.291kJ/mol and is lower than the value for struvite-II has 1.561 kJ/mol. This confirms the oxidation of organics from ANWW by HFO process.

The DTA analysis showed a sharp endothermic peak at 122.08°C, it may be attributed to the release of water of crystallization along with NH_4^+-N. The decomposition at this stage with a weight loss was 13%. Thus, the sharpness of endothermic peak in DTA may be attributed to good crystallinity of the struvite crystal. The sharp endothermic peak at 145.53°C for the Struvite II crystal as shown in Fig.7 (b) is assigned to weight loss by 11.28%.Some minor endothermic peaks observed at 325 °C and 400-450 °C, may be attributed to the presence of organic impurities .These peaks are missing in Struvite I as shown in Fig. 7(a). DTA study concludes the presence of good degree of crystallinity in the Struvite crystals I and II, and the purity of the struvite was enhanced by the HFO process.

The DSC thermograms for Struvite crystals I and II are shown in Fig. 8(a) and 8(b). The Struvite I and Struvite II crystals showed the characteristic exothermic peak at 127.01°C, which may be attributed to the elimination of water of crystallization and ammonia molecules during struvite decomposition.

FT-IR analysis of struvite crystals formed from ANWW and $[ANWW]_{HFO}$

The recovered struvite crystals were characterised for the identification of functional groups by FT-IR analysis. Fig. 9 show the FT-IR spectra of struvite crystals formed from ANWW and $[ANWW]_{HFO}$. In Fig. 9, the stretching absorption peak observed at 3249.7cm^{-1} confirmed the presence of N-H functional group and the absorption peak at 1657.0 cm^{-1} is attributed to the N-H bending vibration. The absorption peaks observed at 1513.4cm^{-1} and 1354.3 cm^{-1} are due to the presence of N-

H asymmetric stretching vibration in ammonium ion. The absorption peak at 567.3 cm^{-1} may be attributed to metal-oxygen bond. The absorption peak at 2105.19 cm^{-1} is due to H-O-H stretching vibration in the cluster of water molecules. The absorption peak at 1016.8 cm^{-1} is due to the presence of stretching vibration in ionic phosphate (O-P-O) stretching. The absorption peaks at 760.1cm^{-1} and 887.6 cm^{-1} are due to the rocking of N-H bond vibrations. The Struvite crystal II formed from ANWW showed more peaks in the aromatic region of the spectrum. This may be attributed to the presence of organic compounds along with struvite components while such peaks are missing in the Struvite I.[35-37]

X-Ray Diffraction and Scanning Electron Microscopic Analysis of struvite:

XRD and SEM analyses were performed for the recovered struvite crystals to identify their crystalline nature and to capture their morphology. Fig. 10(a) and 10(b) show the SEM images of recovered Struvite I and Struvite II crystals. It was found that the struvite crystal II belong to orthorhombic space lattice system with the average size of ~100 µm. The Struvite crystal I showed coffin-shape with average size of ~5µm. The difference in size of Struvite crystals I and II may be due to the presence of organic impurities. The larger size of Struvite crystal II is due to the agglomeration of struvite crystals with organic molecule during precipitation process from ANWW. Fig. 10(c) and 10(d) show the XRD patterns of struvite crystals I and II. The 2θ values observed with the reference of JCPDS (Card No 1-077-2303)[38] indicate the characteristic orthorhombic crystalline planes in both the recovered Struvite crystals I and II. But in Struvite crystal II, noise peaks observed indicates the inclusion of organic impurities within the crystal lattice system. However, the XRD spectrum showed less noise peaks in Struvite I which may be due to the removal of organic pollutants by HFO process.[17]

Conclusions

The high concentrated NH_4^+–N containing wastewater discharged from chemical industry was treated by HFO process using $^{\bullet}OH$ generated from Fe^{2+}/H_2O_2 and $NPAC/O_2$ for the destruction of organic compounds in wastewater. The maximum percentage removal of NH_4^+-N was 94-96% in MAP process after the removal of COD by 78-86%; BOD by 69-75% and TOC by 64-70% in HFO process. The molar ratio of NH_4-N^+:Mg^{2+}:PO_4^{3-} for the maximum yield of struvite precipitation was found to be 1:1.4:1.4.

The instrumental analyses such as TGA, FT-IR and XRD confirmed the recovered crystals were struvite and the pure form of struvite was recovered after following HFO process. The precipitation of struvite followed pseudo second order kinetic model with kinetic constant, 0.365 L mol^{-1} min^{-1}.

Acknowledgements

The authors acknowledge CSIR-CLRI, India for granting financial support from STRAIT Project (CSC 0201) to carry out this research work.

References

1 G.E. Diwani, S.E. Rafie, N.N.E. Ibiari, H.I. El-Aila, Desalination, 2007, 214, 200–214.

2 O. Tunay, I. Kabdasli, D. Orhon, S. Kolcak, Water Sci. and Technol., 1997, 36, 225–228.

3 J.N. Galloway, W.H. Schlesinger, H. Levy, A. Michaels, and J.L. Schnoor, Global Biochem. Cyc., 1995, 9, 235-252.

4 U. Welander, T. Henrysson, T. Welander, Water Res., 1998, 32, 1564–1570.

5 B.Molinuevo, M.C. García, D.Karakashev, I. Angelidaki, Bioresour.Technol., 2009, 100, 2171-2175.

6 P. Nigam, G. Armour, I.M. Banat, D. Singh, R. Marchant, 2000, Biotechnology, 2000, 72, 219-226.

7 A. Bonmati, X. Flotats, Waste Manage. (Oxford), 2003, 23, 261–272.

8 K.W. Kim, Y.J. Kim, I.T. Kim, G.I. Park, E.H. Lee, Water Res., 2006, 40, 1431–1441.

9 B.Y. Jeong, S.H. Song, K.W. Baek, I.H. Cho, T.S. Hwang, Polymer (Korea), 2006, 30, 486–491.

10 Y.H. Liu, J.H. Kwag, J.H. Kim, C.S. Ra, Desalination, 2011, 277, 364–369.

11 H. Siegrist, Water Sci. and Technol., 1996, 34(1-2) 399-406.

12 R. Gonzalez Poncer, D.M.E. Garcialopez, Agrochimica, 2007, 51, 301–308.

13 K. Yetilmezsoy, Z.S. Zengin, J. Hazard. Mater., 2009, 166, 260–269.

14 N.O. Nelson, Masters Thesis, Dept. of Soil Science, 2000, North Carolina State University, Raleigh, NC, USA.

15 G.K. Ghosh, K.S. Mohan, A.K. Sarkar, Nutr. Cycl. Agroecosyst., 1996, 46, 71–79.

16 M.R. Gaterell, R. Gay, R. Wilson, R.J. Gochin and J.N. Lester, Environ. Technol., 2000, 21, 1067-1084.

17 X.D. Hao, C.C. Wang, L. Lan and M.C.M. Van Loosdrecht, Water Sci. and Technol., 2008, 58, 1687–1692.

18 Nicolaos Ch. Bouropoulos, Petros G. Koutsoukos, J. Cryst. Growth., 2000, 213,381–388.

19 M.M. Rahman, Y.H. Liu, J.H. Kwag, C.S. Ra, J. Hazard. Mater. 2011, 186, 2026–2030.

20 D.G. Chirmuley, Water (J. Aust. Water Assoc.), 1994, 21–23.(4)

21 M.Turker and I.Celen, J. Eng. Environ. Sci., 2010, 34, 39 – 48.

22 Stratful, M.D. Scrimshaw and J.N. Lester, Water Res., 2001, 35, 4191-4199.

23 J.H. Cho, J.E. Lee, C.S. Ra, J. Anim. Sci. Technol., 2009, 51, 337–342.

24 S. Karthikeyan, M. Ezhil Priya, R. Boopathy, M. Velan, A. B. Mandal, G. Sekaran, Environ.Sci. Pollution Res. 2012, 19, 1828–1840.

25 APHA, AWWA, WEF, Standard methods for the examination of water and wastewater, 1998, 20th edn.

26 S. Kathikeyan and G. Sekaran, Phys.Chem.Chem.Phys., 2014, 16, 3924-3933

27 E.M. Siedlecka, P Stepnowski , Environ. Sci. Pollut. Res., 2009, 16, 453–458.

28 S. Karthikeyan, A. Titus, A. Gnanamani, A.B. Mandal, G. Sekaran, Desalination, 2011, 281, 438-445..

29 K.N. Ohlinger, T.M. Young, E.D. Schroeder, J. Environ. Eng., 1999, 125, 730–737.

30 K. S. Le Corre, E. Valsami-Jones, P. Hobbs, and S. A. Parsons, Crit. Rev. Env. Sci. Tec., 2009, 39, 433–477.

31 M.Türker, I. Çelen, Bioresour.Technol., 2007, 98, 1529-1534.

32 C.Wang, X.Hao, G.Guo and MCM.Van Loosdrecht. Chem. Eng. J., 2010, 159, 280-283.

33 M.I.H. Bhuiyan, D.S.Mavinic and F.A. Koch, Chemosphere. 2008,70,1347-1356.

34 R.L.Frost, M.L.Weier, K.L.Erickson, J. Therm. Anal. Calorim., 2004, 76, 1025-1033.

35 G. Kurtulus A.C. Tas, Mater. Lett., 2011, 65, 2883- 2886.

36 B. Soptrajanov, V. Stefov, H.D. Lutz, B. Engelen, J. Mol. Struct., 2005, 752, 60-67.

37 Mathematics, Physics and Chemistry: Spectroscopy of Emerging Materials: Netherlands, Springer, 165, 299-308.

38 E. L.Foletto, W. R. B. D.Santos, M. A.Mazutti, S. L.Jahn, A.Gündel, Mater. Res., 2013, 16, 242-245.

Table 1 Characteristics of Ammoniacal nitrogen containing wastewater (ANWW) at different stages of treatment

Parameters	Initial wastewater	Wastewater after sand filtration
pH	0.82	0.87
Chemical Oxygen Demand , COD	8720	8530
Biochemical Oxygen Demand, BOD_5	2420	2390
BOD_5/COD	0.27	0.273
Total Organic Carbon , TOC	1662	1658
Ammoniacal nitrogen , NH_4^+ -N	1915	1905
Total Kjeldhal nitrogen, TKN	1982	1977
Total Solids	9647	9598
Total Dissolved Solids	9420	9412
Total Suspended Solids	227	106

All the values except pH and BOD_5/COD are expressed in mg/L

Table 2 Kinetic parameters of COD removal from ANWW during HFO process

	Pseudo first order			Pseudo second order		
	$k_1(min^{-1})$	R^2	χ^2	$k_2(Lmol^{-1} min^{-1})$	R^2	χ^2
COD removal	0.088	0.809	0.078	$2.575x10^{-5}$	0.997	0.0023

Table 3 Variation in solution pH during the addition of MAP reagents during struvite precipitation

Stoichiometric molar ratio (NH_4^+-N:Mg^{2+}:PO_4^{3-})	Solution pH after the addition of $Na_2HPO_4.2H_2O$	Solution pH after the addition of MgO
1.0:1.0:1.0	5.92	8.33
1.0:1.1:1.1	5.87	8.31
1.0:1.2:1.2	5.74	8.28
1.0:1.3:1.3	5.68	8.35
1.0:1.4:1.4	5.62	8.32
1.0:1.5:1.5	5.58	8.32

Table 4 Kinetic parameters on the removal of NH_4^+-N from $[ANWW]_{HFO}$

	Pseudo first order			Pseudo second order		
	$k_1(min^{-1})$	R^2	χ^2	$k_2(Lmol^{-1}min^{-1})$	R^2	χ^2
Ammoniacal nitrogen removal	0.001	0.965	0.028	0.365	0.987	0.0026

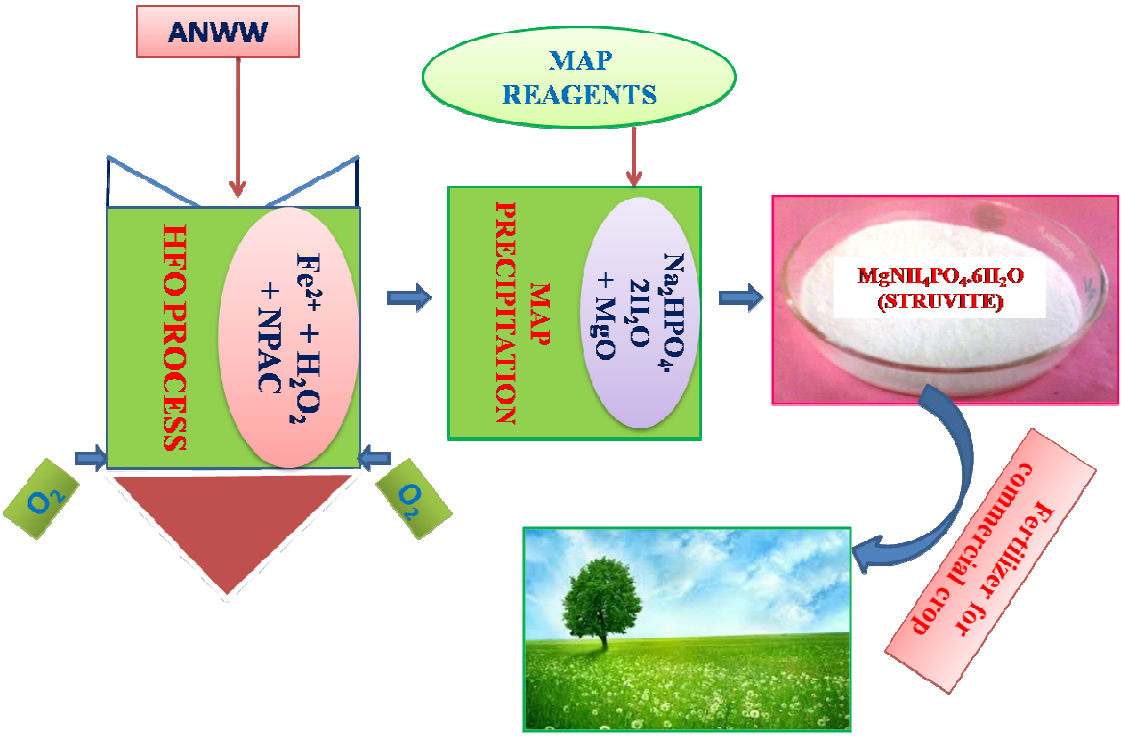

Fig.1 Graphical representation of integrated HFO and MAP processes

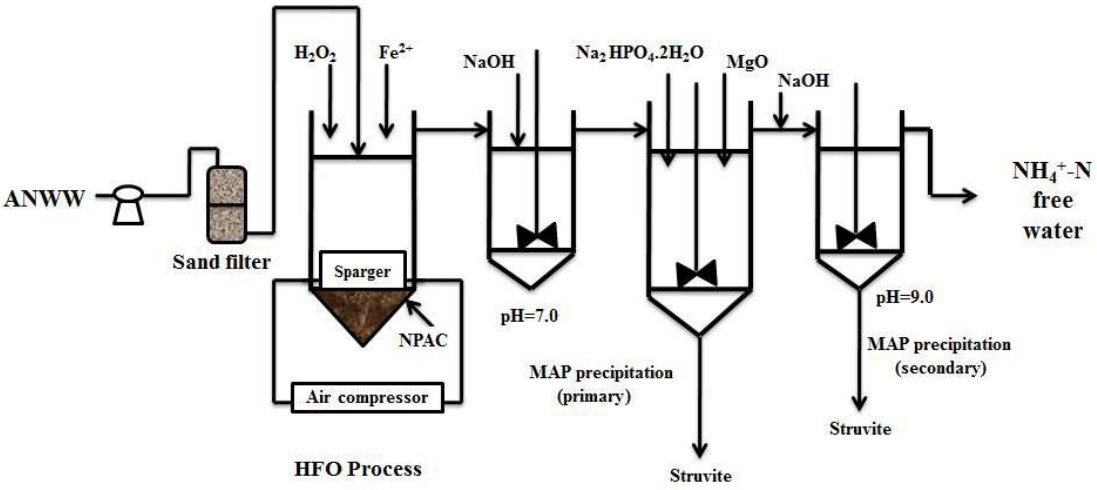

Fig. 2 Schematic representation of integrated HFO and MAP processes

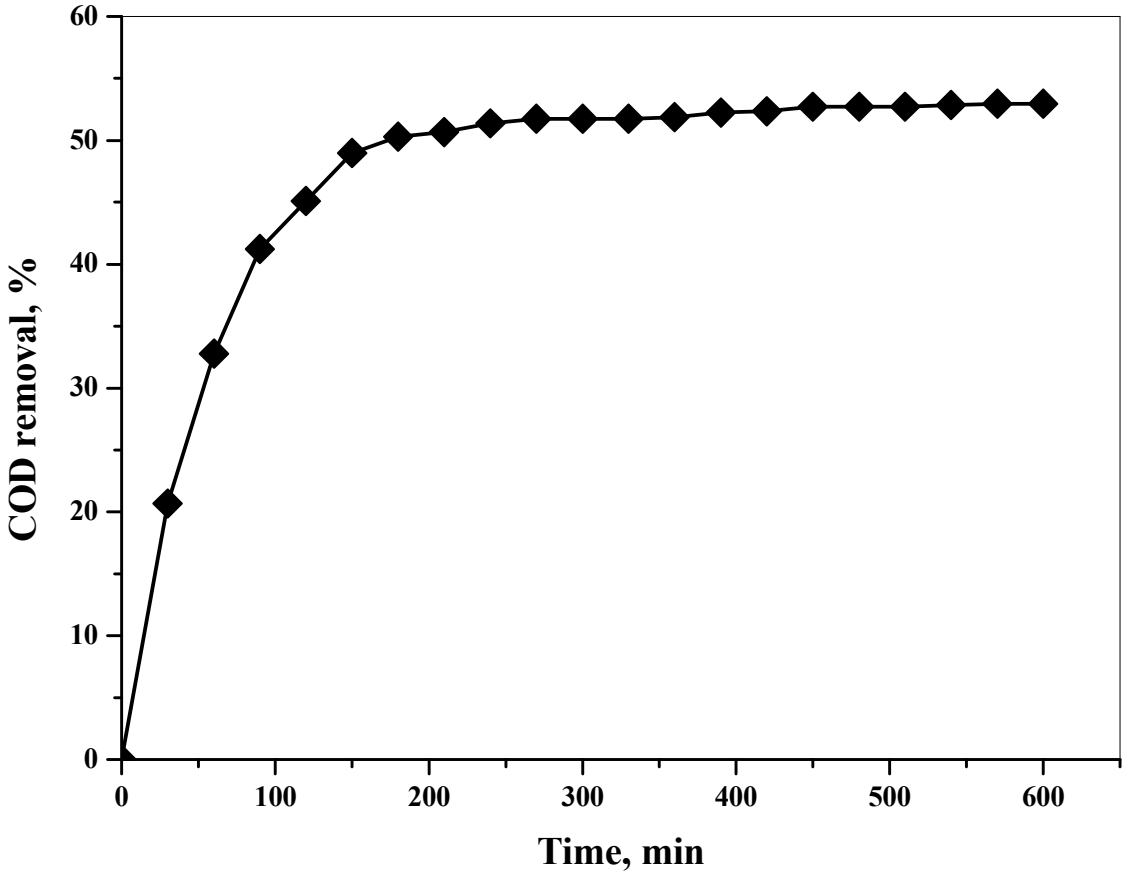

Fig. 3 Effect of time on COD removal in HFO process

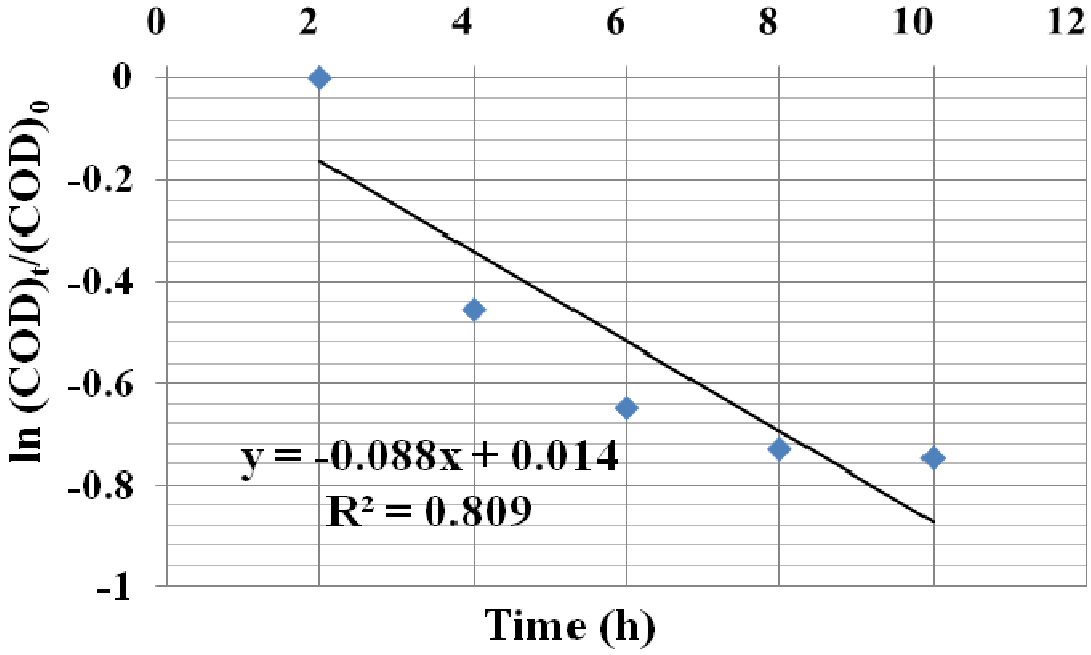

Fig. 4(a) Pseudo first order rate kinetic model for the COD removal in HFO process

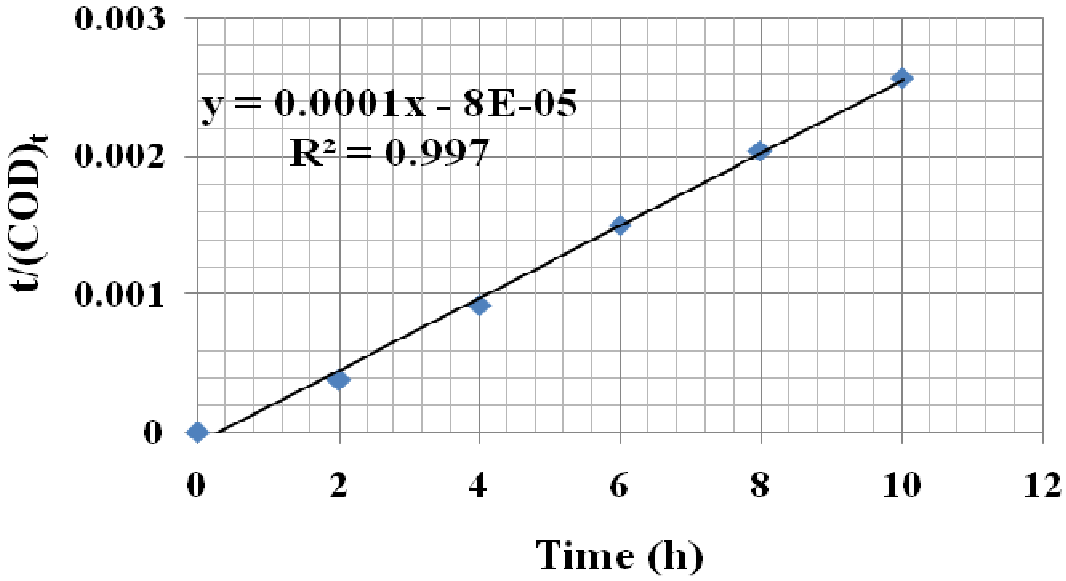

Fig. 4(b) Pseudo second order rate kinetic model for the COD removal in HFO process

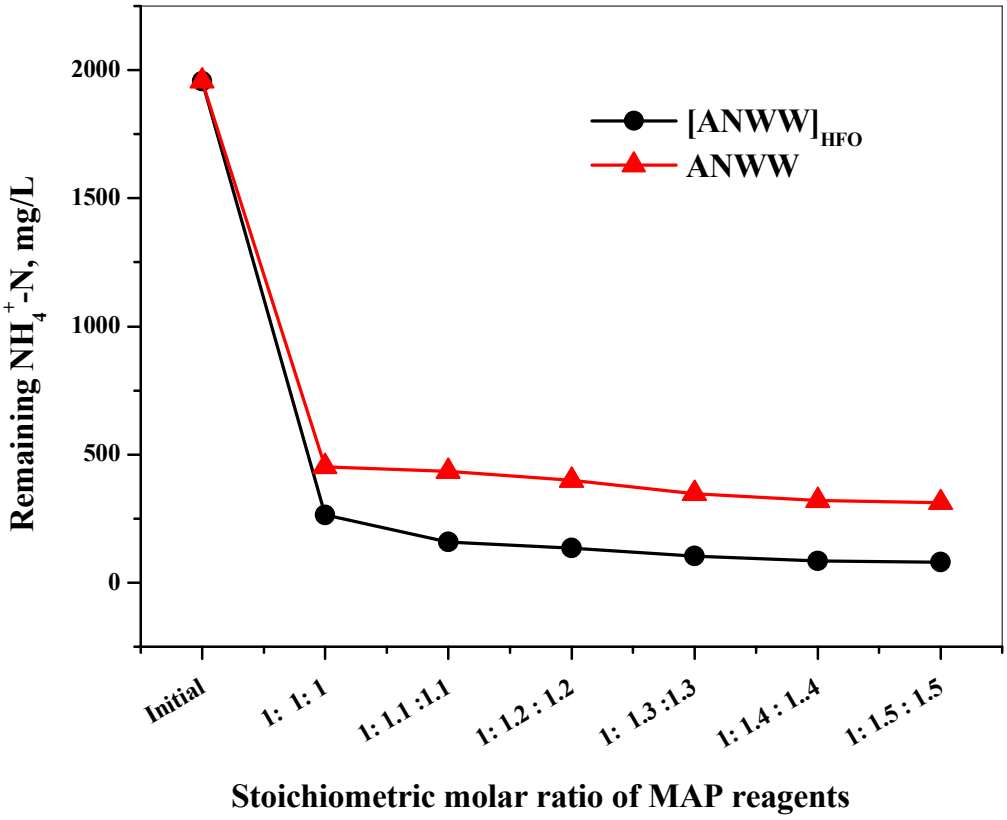

Fig. 5(a) Remaining NH_4^+-N in wastewater at different stoichiometric molar ratio of MAP reagents

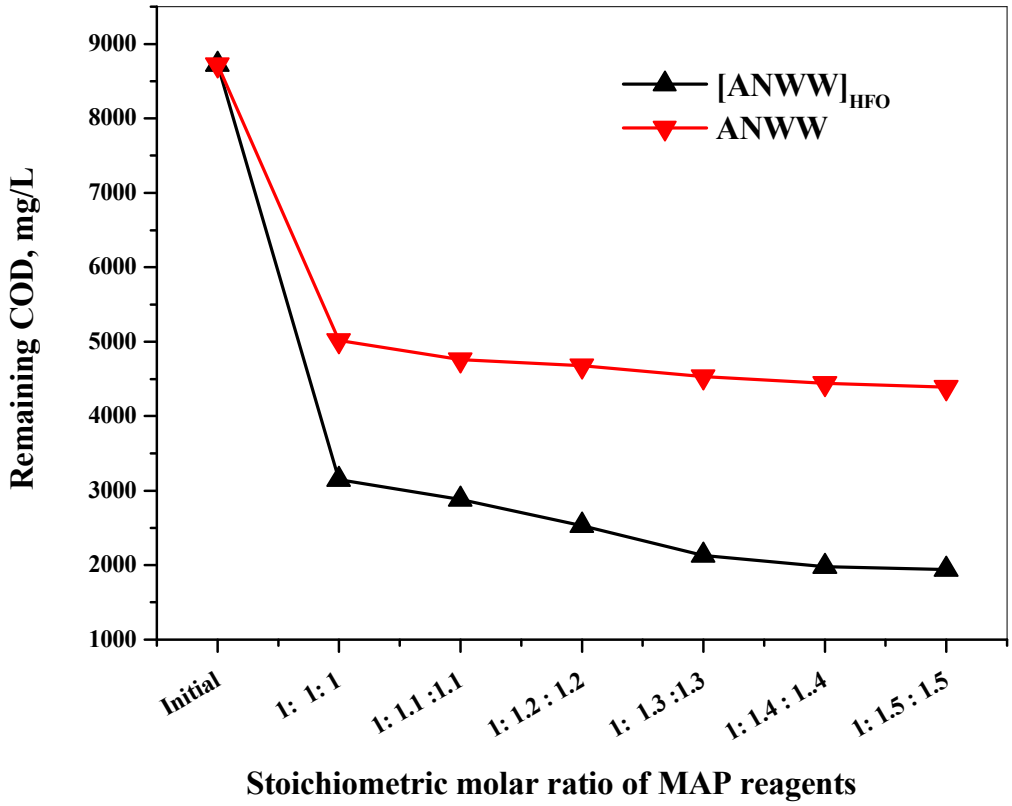

Fig. 5(b) Remaining COD in wastewater at different stoichiometric molar ratio of MAP reagents

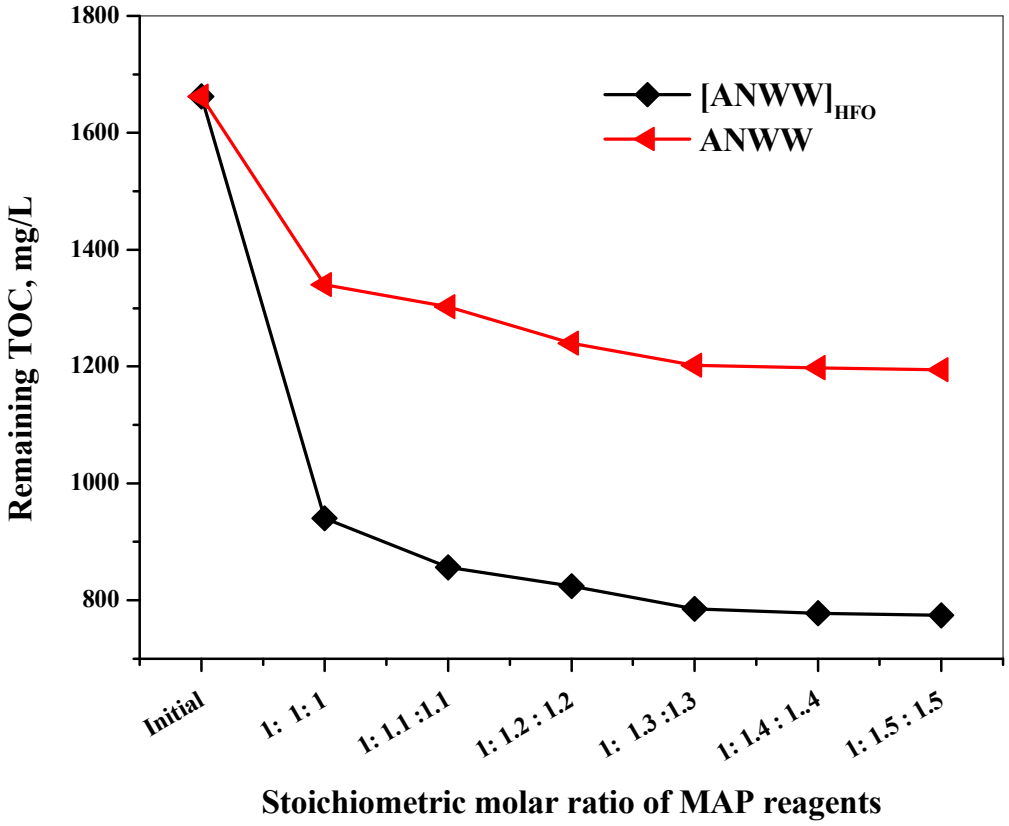

Fig. 5(c) Remaining TOC in wastewater at different stoichiometric molar ratio of MAP reagents

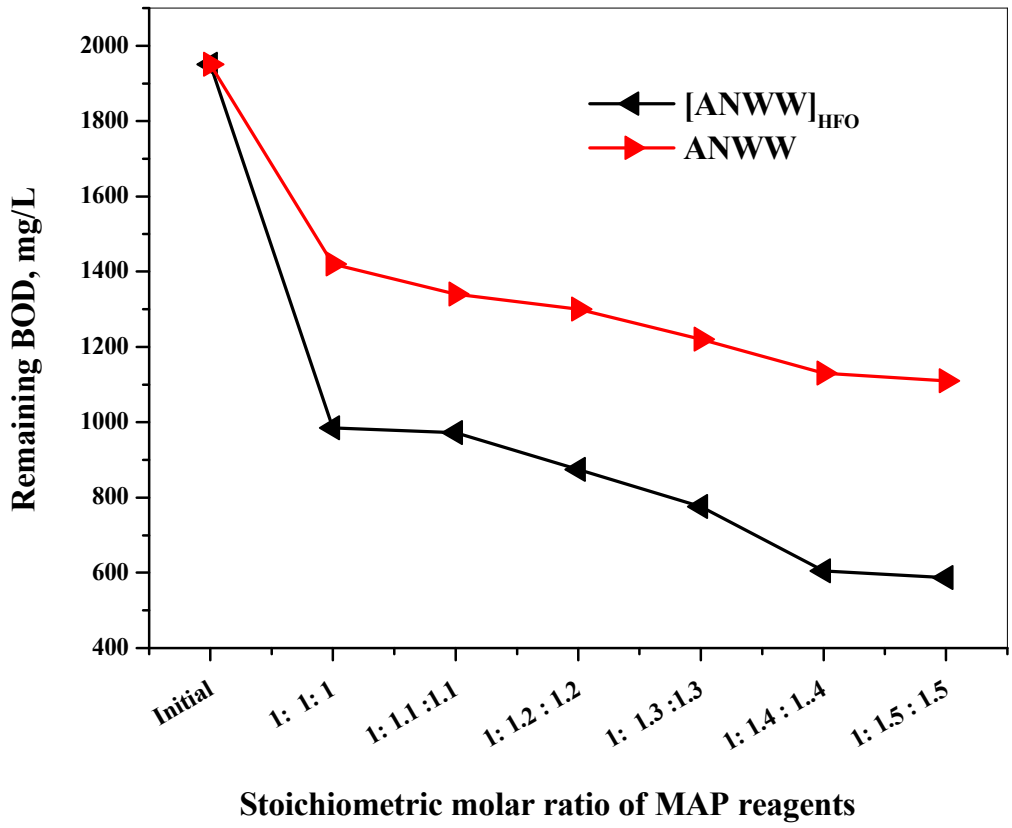

Fig. 5(d) Remaining BOD in wastewater at different stoichiometric molar ratio of MAP reagents

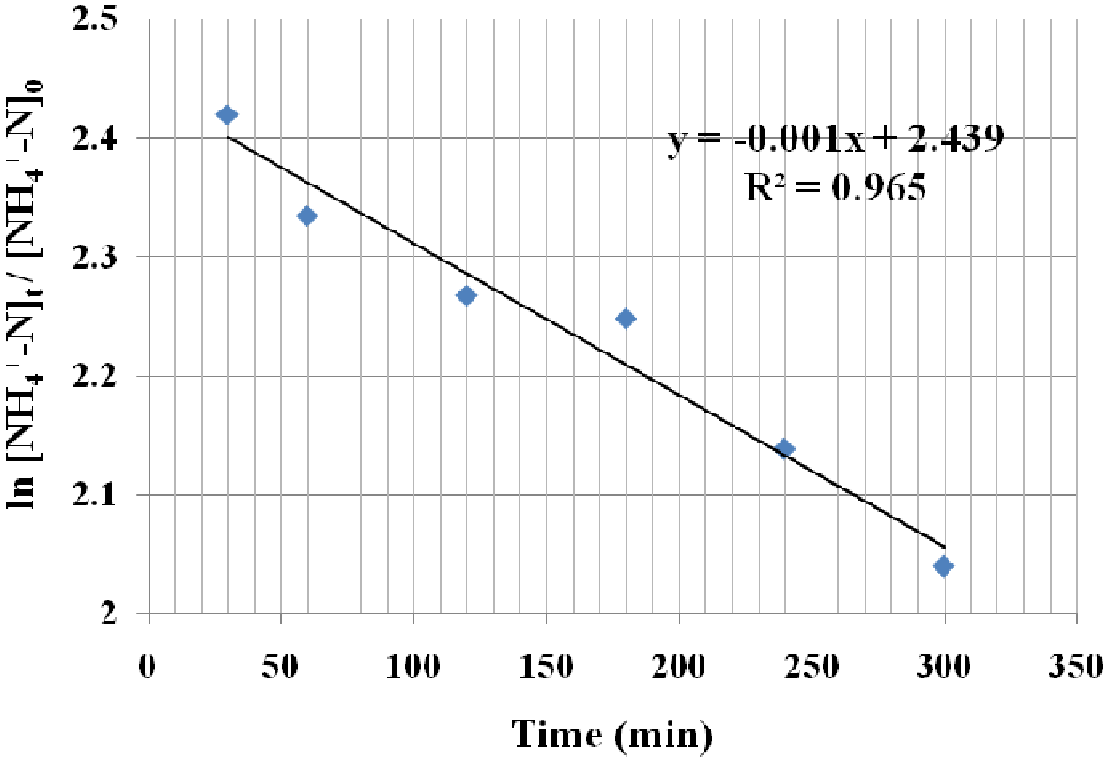

Fig. 6(a) Pseudo- first order rate kinetic model for NH_4^+-N removal as struvite crystals

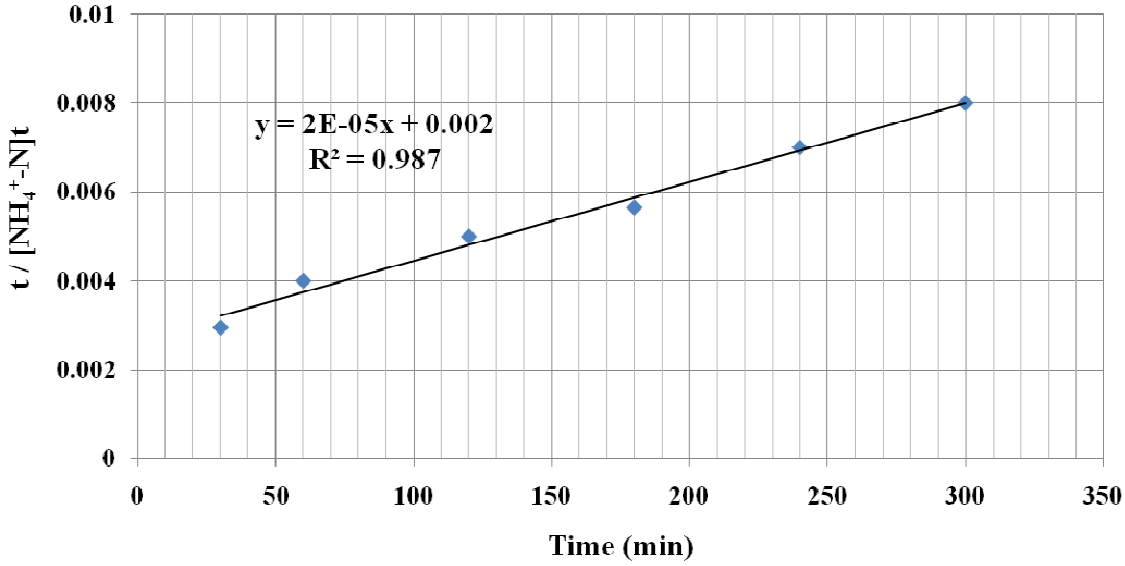

Fig. 6(b) Pseudo- second order rate kinetic model for NH_4^+-N removal as struvite crystals

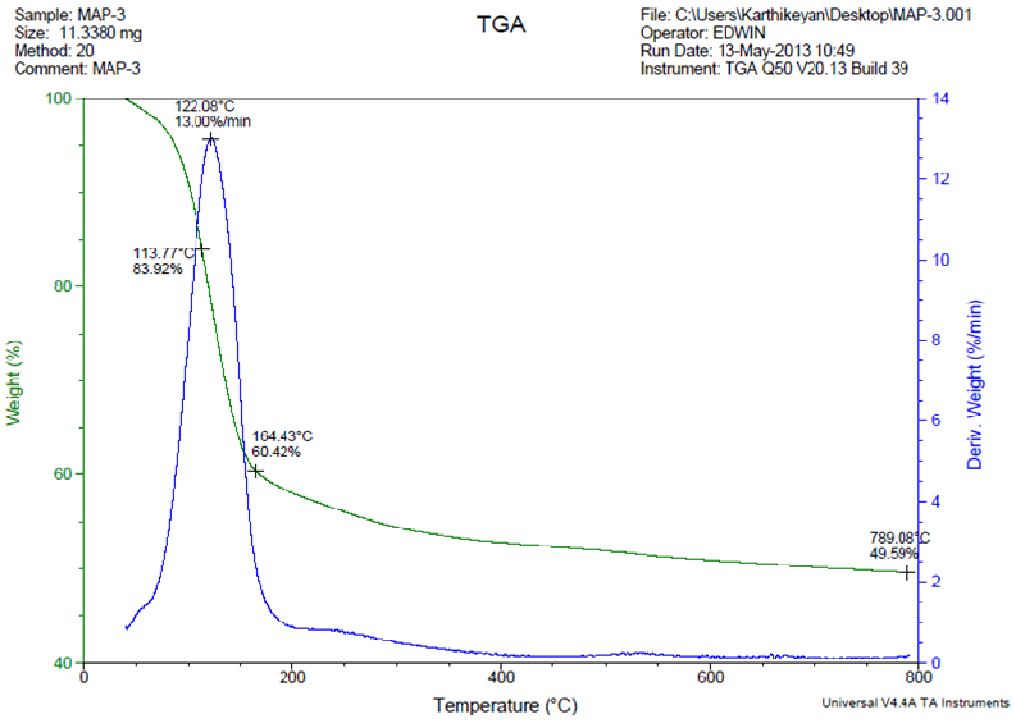

Fig. 7(a) TGA for Struvite crystal I recovered from $[ANWW]_{HFO}$

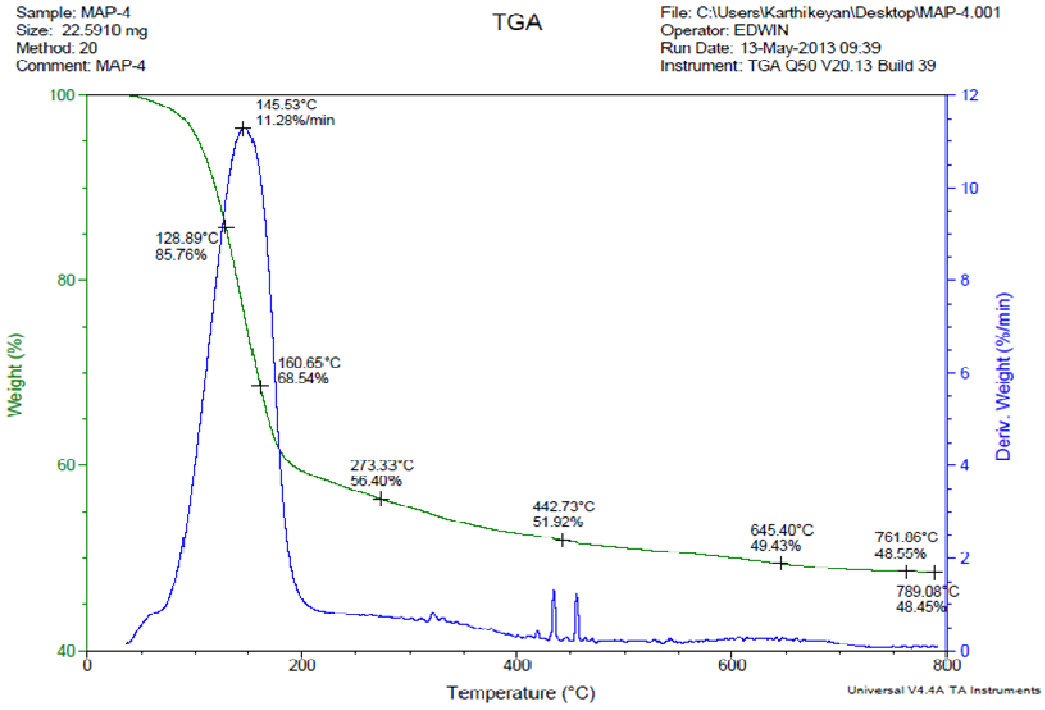

Fig. 7(b) TGA for Struvite crystal II recovered from ANWW

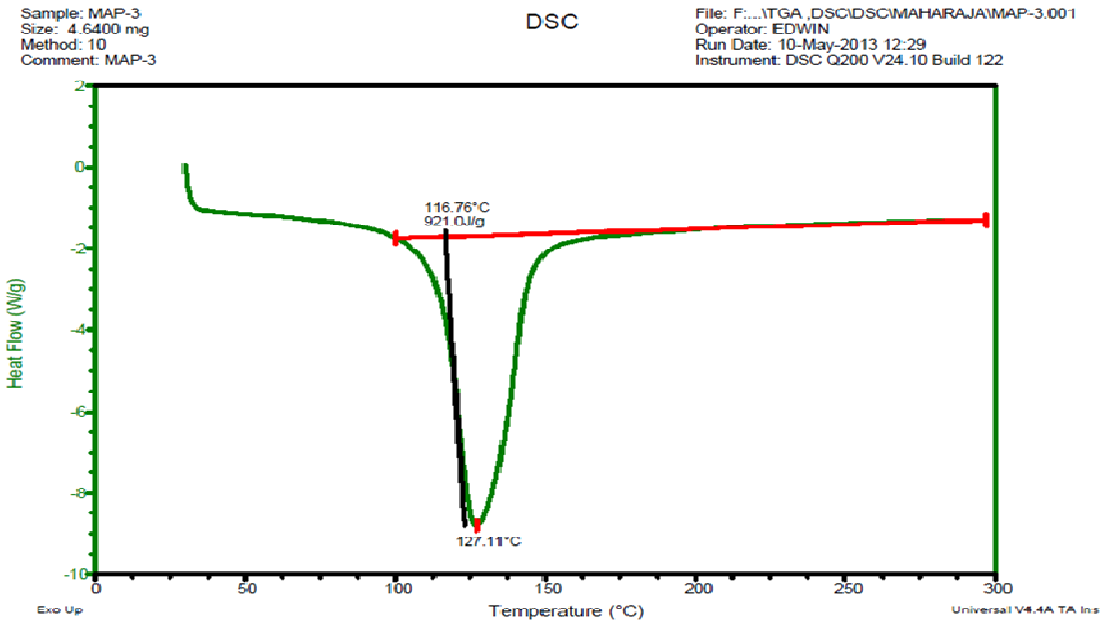

Fig. 8(a) DSC spectrum of Struvite crystal II recovered from ANWW

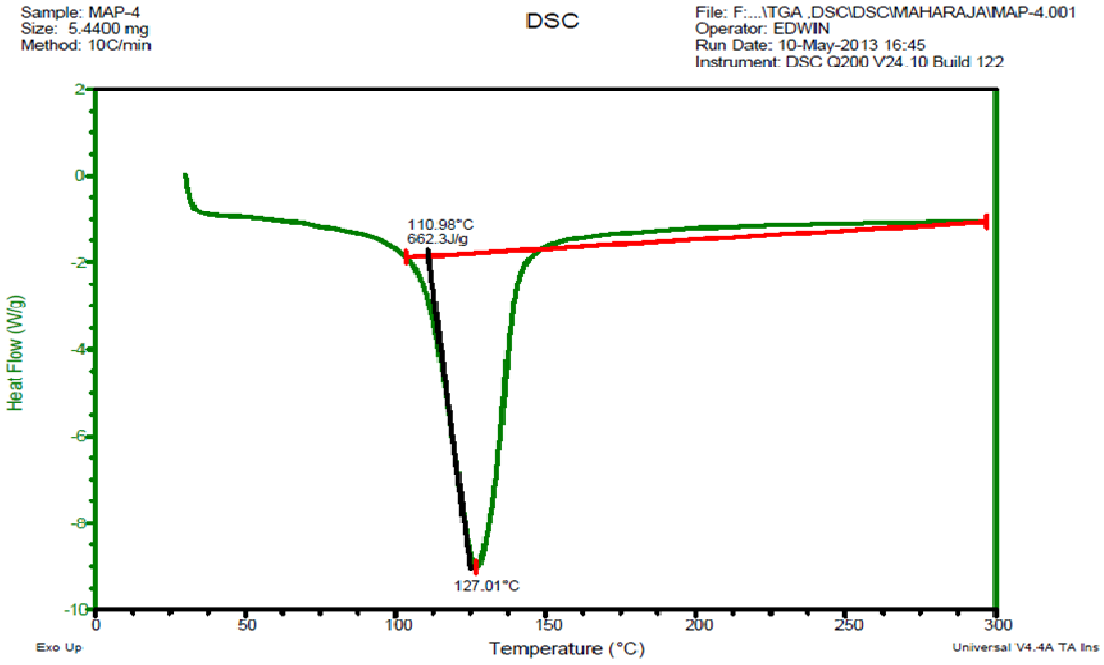

Fig. 8(b) DSC spectrum of Struvite crystal I recovered from $[ANWW]_{HFO}$

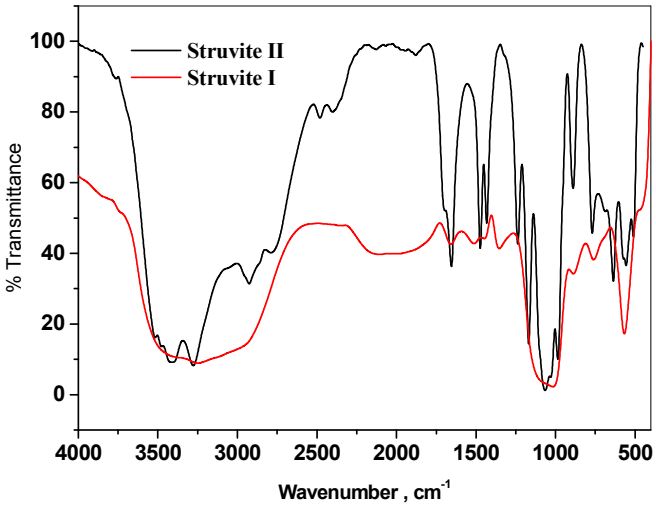

Fig. 9 FT-IR spectra of Struvite crystals I and II from $[ANWW]_{HFO}$ and ANWW

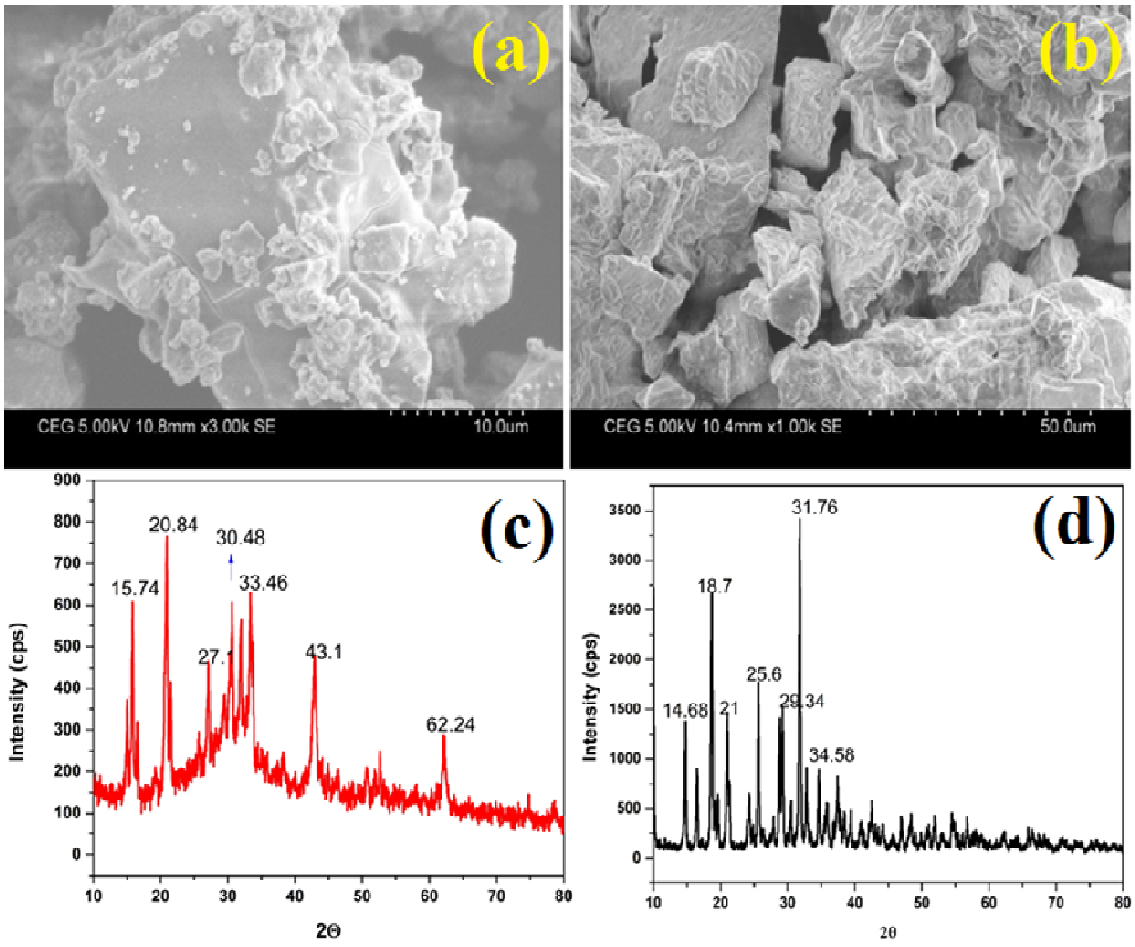

Fig. 10(a) SEM image of Struvite crystal II recovered from ANWW, **(b)** SEM image Struvite crystal I recovered from $[ANWW]_{HFO,}$ **(c)** XRD spectrum Struvite crystal II recovered from ANWW, **(d)** XRD spectrum of SEM image Struvite crystal I recovered from $[ANWW]_{HFO}$.

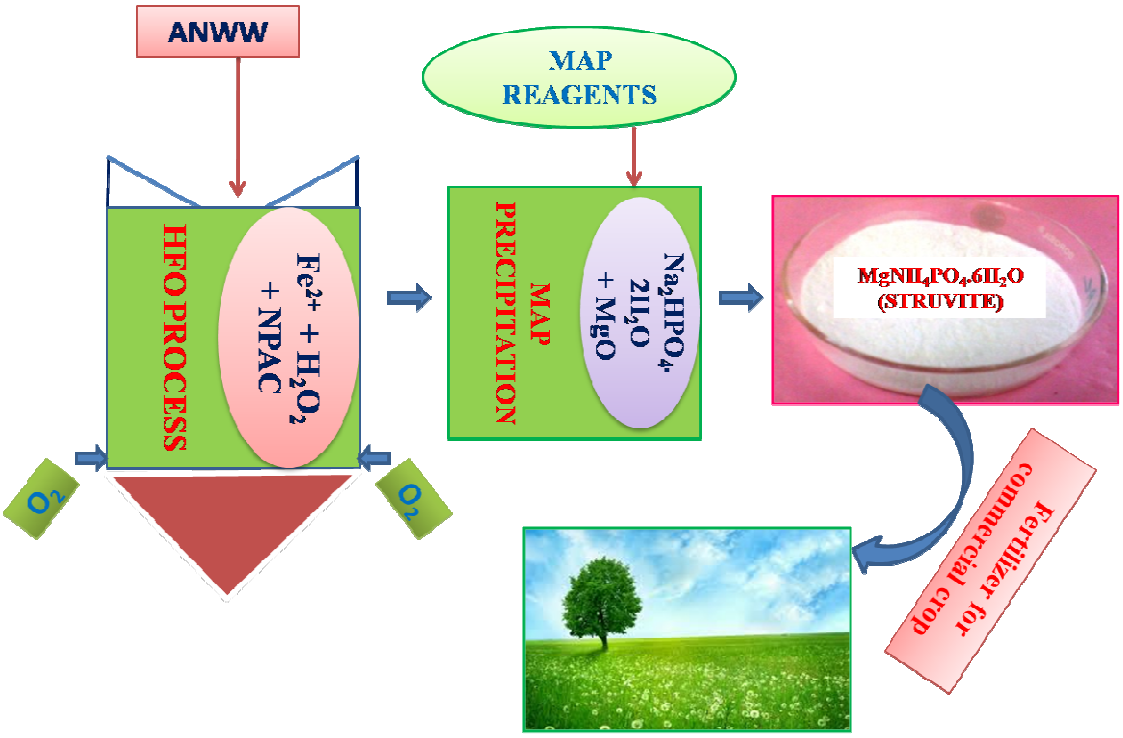

Graphical representation of integrated HFO and MAP processes